Journal of Materials Chemistry C

Accepted Manuscript

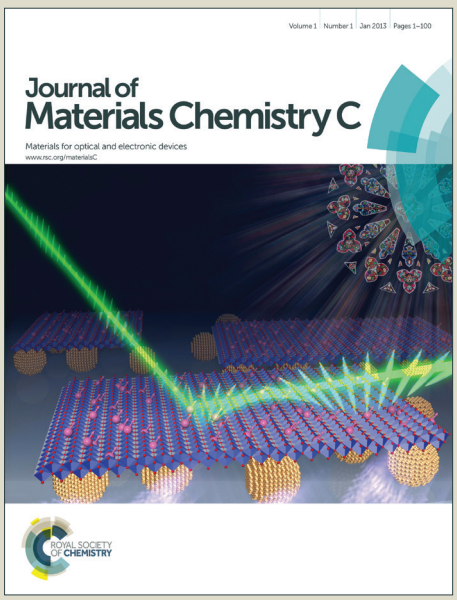

ROYAL SOCIETY OF CHEMISTRY

www.rsc.org/materialsC

Journal of Materials Chemistry C

ARTICLE

A Super Energy Transfer Process Based S-shaped Cluster in $ZnMoO_4$ Phosphors: Theoretical and Experimental Investigation

Received 00th January 20xx,
Accepted 00th January 20xx

DOI: 10.1039/x0xx00000x

www.rsc.org/

Weiguang Ran,[a] Lili Wang,[a] Wenwen Zhang,[a] Feiyang Li,[b] Haiyan Jiang,[a] Weina Li,[a] Linghao Su,[a] Ruizhi Houzong,[a] Xiaohua Pan,[a] Jinsheng Shi*[a]

Efficient energy transfer from sensitizer to activator in phosphors is very important for white LEDs. Bi^{3+} and Eu^{3+} co-doped red phosphor is a potential alternative for white LEDs. However, energy transfer from Bi^{3+} to Eu^{3+} ions is still not efficient enough in most cases. Here we have found that every six Zn sites forming an S-shaped cluster in $ZnMoO_4$ crystal. Two Zn(2) sites will be occupied preferentially in $ZnMoO_4$ according to the comparison between calculated and experimental A band positions of Bi^{3+} in $ZnMoO_4$ host. Considering the S-shaped cluster and site occupation preference, a super energy transfer process from Bi^{3+} to Eu^{3+} ions is proposed. The distance between Bi^{3+} and Eu^{3+} ions can be controlled by their total doping concentrations. When their total molar concentration is beyond 1/6, Bi^{3+} and Eu^{3+} began to sit two adjacent Zn(2) sites. Thus, the new super energy transfer from Bi^{3+} to Eu^{3+} emerged due to adjacent Bi^{3+} and Eu^{3+} ions. When excited at 331 or 350 nm, which is assigned to $^1S_0 \rightarrow {}^3P_1$ transition of Bi^{3+}, the phosphor emits intense red light. The relative intensity is about 6 times higher than that with ordinary transfer process. It gives a good example to utilize the site occupation preference and provides a new way to design efficient phosphors.

1. Introduction

Nowadays, white light-emitting diodes (LEDs) as the next generation of illumination technology have attracted increasing attentions due to high efficiency, long lifetime and environment-friendly characteristics.[1-2] Phosphor-converted LED technique is the main approach to produce solid-state illumination devices. The conventional phosphor-conversion white LED is the conjunction of an InGaN blue LED with a cerium-doped yttrium aluminum garnet (YAG: Ce^{3+}) phosphor which was first proposed in 1997.[3] However, YAG: Ce^{3+} phosphor is of poor color-rendering ability (Ra) because of weak emission in the red spectral region. One of the most-used strategies to solve this problem is to introduce a red phosphor with strong blue absorption. But up to now, most commercial red phosphors are based on nitrides and oxynitrides with harsh preparation conditions such as $Ba_2Si_5N_8:Eu^{2+}$, $CaAlSiN_3:Eu^{2+}$ and $Sr[LiAl_3N_4]:Eu^{2+}$.[4-6] And they still have some limitations in terms of red color purity, efficiency and stability.[6] In addition, white light can be generated by combining a near-UV LED chip with red, green and blue phosphors, which may solve the above problems. Therefore, the development of efficient near-UV or blue pumped red phosphor is very important to create a warm WLED.

Eu^{3+} activated molybdate are potential red emitting phosphors because of narrow $^5D_0 \rightarrow {}^7F_2$ transition of Eu^{3+} at about 620 nm.[7-9] However, the broad excitation band for Mo^{6+}-O^{2-} charge transfer band usually lies in the 250-350 nm, resulting in weak absorption of light in the near UV region of the phosphor. Bi^{3+} ion have been broadly used as a sensitizer for Eu^{3+} in phosphors.[10-11] According to our prediction of the position of Bi^{3+} $^1S_0 \rightarrow {}^3P_1$ transition in $ZnMoO_4$, it is likely to appear an excitation band to enhance the absorption of $ZnMoO_4:Eu^{3+}$ in the near UV region. However, how to improve the energy transfer efficiency from Bi^{3+} to activator such as Eu^{3+} is still a challenge.[12] As we all known, the distance between sensitizer and activator are important factors that affecting energy transfer between them. Furthermore, the host lattice environment of luminescent materials is a hotspot because of their significance for the understanding of light-emitting mechanism.[13-16] Nowadays, multi-emissions from different sites have been reported but how to predict the location of the dopant is still a challenging problem.

The efficient energy transfer from sensitizers to activators is very important for improving the luminescence behaviour of phosphors. The appropriate distance between activators and sensitizers will provide a possibility for efficient energy process, but how to control the distance is still very difficult. $ZnMoO_4$ is an efficient host matrix for rare earth luminescence materials.[17-19] In this work, it was found that every six Zn sites in $ZnMoO_4$ form an S-shaped cluster. The environmental factor *he* of three kinds of Zn sites were calculated based on our previous work. According to the semi-empirical formula, it can be concluded that Bi^{3+}, Eu^{3+} and Tb^{3+} ions will enter Zn(2) site in $ZnMoO_4$. When the concentration of Eu^{3+} or Tb^{3+} ions is over than 1/6, concentration quenching occurred due to energy immigration between close Eu^{3+} or Tb^{3+} ions. On account of the S-shaped cluster of Zn sites and site occupation preference in

[a] Qingdao Agricultural University, Qingdao 266109, People's Republic of China.
[b] College of Chemistry, Chemical Engineering and Material Science, Shandong Normal University, Jinan 250014, People's Republic of China.

† Footnotes relating to the title and/or authors should appear here.
Electronic Supplementary Information (ESI) available: [details of any supplementary information available should be included here]. See DOI: 10.1039/x0xx00000x

$ZnMoO_4$, the position of Bi^{3+} and Eu^{3+} ions can be controlled by changing their total concentration and a super energy transfer process from Bi^{3+} to Eu^{3+} was realized. When the total concentration of Bi^{3+} and Eu^{3+} ions is beyond 1/6, the super energy transfer process from Bi^{3+} to Eu^{3+} occurred due to short distance between them. Thus, a red emitting phosphor with broad excitation band was obtained and a new way to investigate site occupation was proposed.

2. Experimental section

2.1 Materials and preparation

$ZnMoO_4:Eu^{3+}$, $ZnMoO_4:Tb^{3+}$ and $ZnMoO_4:Bi^{3+}$, Eu^{3+} phosphors with different concentrations were synthesized by a traditional high temperature solid-state reaction in air atmosphere. The raw materials are ZnO (99%), Tb_4O_7 (99.99%), Eu_2O_3 (99.99%), Bi_2O_3 (99.9%), and MoO_3 (99%). The starting materials were weighed according to stoichiometric ratio and well mixed in agate mortar. The mixtures were put into alumina crucible and calcined in muffle furnace at 700-800°C for 3 h, and then the white powder phosphor was obtained.

2.2 Characterization

The structures of $ZnMoO_4$ samples were determined using a Bruker D8 Advance X-ray diffractometer (Cu $K\alpha_1$ radiation, λ=0.15406 nm) with radiation at a 0.01° (2θ) /0.5 s scanning step. Structural refinements were performed by the GSAS (General Structure Analysis System) program. The photoluminescence excitation (PLE) and emission (PL) spectra were recorded with a Hitachi F-4600 spectrophotometer equipped with a 150 W xenon lamp as an excitation source.

3. Results and discussion

3.1 Crystal structure, Phase Identification and Purity.

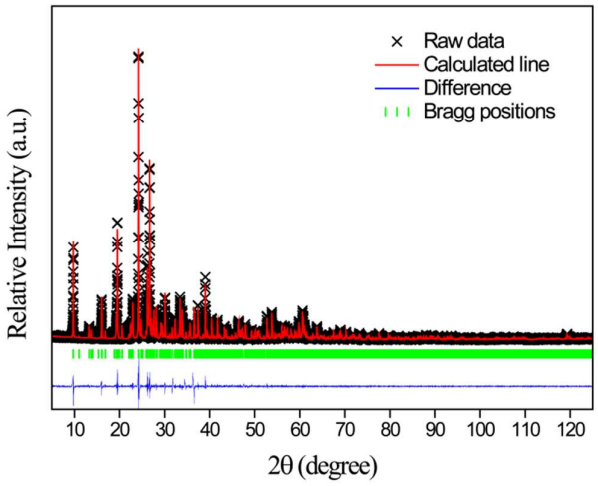

Fig. 1 Final Rietveld refinement profiles of $ZnMoO_4$.

The structure refinement of the $ZnMoO_4$ sample was performed using the GSAS software package and the initial parameters of refinement for $ZnMoO_4$ sample were referred from the single crystal data of $ZnMoO_4$ (ISCD-411378). The refined results are given in Table 1, and the final refinement patterns are shown in Fig. 1. Pure $ZnMoO_4$ sample crystallized in space group P-1 with a = 6.966064 Å, b = 8.369425 Å, c = 9.688157 Å, V = 519.77 $Å^3$, α = 96.7396° β = 106.8661° and γ = 101.7387°, which matched well with the reported in literature. [20] All atom positions, fraction factors and temperature factors were refined convergence and well satisfy the reflection condition, with R_p = 7.16%, R_{wp} = 11.19 %, and χ^2 = 3.503.

Table 1 Refined structural parameters of $ZnMoO_4$ obtained from the Rietveld refinement.

Atom	x/a	y/b	z/c	U
Mo1	0.0234(4)	0.2974(1)	0.6271(6)	0.011(9)
Mo2	0.2979(2)	0.3962(2)	0.1579(9)	0.011(2)
Mo3	0.4935(4)	0.0088(6)	0.2430(4)	0.011(1)
Zn1	0.0300(1)	0.1110(1)	0.2857(8)	0.013(6)
Zn2	0.4656(3)	0.3068(2)	0.5126(4)	0.013(2)
Zn3	0.7454(0)	0.3044(0)	0.0889(5)	0.012(9)
O1	0.0262(5)	0.1274(4)	0.7206(4)	0.024(6)
O2	0.0480(5)	0.2639(7)	0.1399(3)	0.015(2)
O3	0.1537(4)	0.4834(3)	0.7532(7)	0.023(2)
O4	0.1404(3)	0.2712(4)	0.4837(1)	0.017(0)
O5	0.2491(0)	0.5634(5)	0.0745(7)	0.021(9)
O6	0.2345(8)	0.7012(2)	0.4585(0)	0.025(9)
O7	0.3499(1)	0.1332(0)	0.3197(6)	0.016(9)
O8	0.3372(2)	0.9074(8)	0.0677(1)	0.018(6)
O9	0.4491(4)	0.1395(7)	0.6502(9)	0.024(9)
O10	0.4462(5)	0.4739(0)	0.3488(5)	0.016(6)
O11	0.4371(1)	0.2910(2)	0.0701(0)	0.020(1)
O12	0.7342(4)	0.1341(2)	0.2387(1)	0.014(9)

Layered arranged Zn-O and Mo-O polyhedra formed $ZnMoO_4$ structure. And the Zn-O polyhedra layers were separated by Mo-O polyhedra layers. Fig. 2(a) shows the Zn-O polyhedra layers in $ZnMoO_4$ crystal structure along the a-direction. As can be seen from the picture, the most prominent structural characteristic of $ZnMoO_4$ is the S-shaped cluster. Fig. 2(b) presents that every six Zn-O polyhedra connecting to become an S-shaped cluster by sharing edges. The S-shaped cluster is completely centrosymmetric. Each two $Zn(2)O_6$ polyhedron connected by shares edges and their relatively distance is only 3.2202 Å. From Fig. 2(c), the coordination environment of the Zn(1), Zn(2) and Zn(3) ions are intuitively displayed. The three different crystal graphically sites have similar symmetry and Zn-O distance. Moreover, the Zn(2) and Zn(3) ions have same coordination number in an approximately octahedral coordination environment. All these make the identification of site occupation in $ZnMoO_4$ more difficult.

Fig. 3 gives the X-ray diffraction patterns of $Zn_{1-x}Eu_xMoO_4$ (x= 0, 1/20, 1/10, 1/6) and $Zn_{1-x}Tb_xMoO_4$ (x= 0, 1/18, 2/18, 3/18) phosphors. It is obvious that all the diffraction peaks can be indexed to the wolframite $ZnMoO_4$ phase (JCPDS 35-0765) with space group P-1 and there are no impurity phases. This indicates that the obtained samples are single-phased and little

Eu^{3+} and Tb^{3+} ions did not cause any significant change in the host structure.

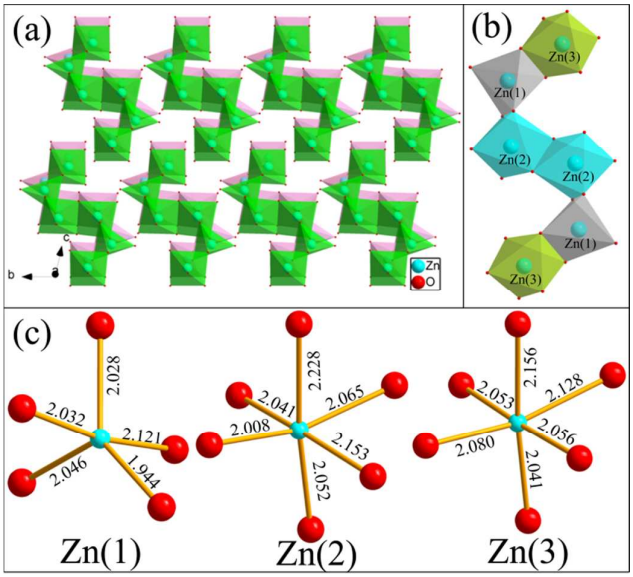

Fig. 2 $ZnMoO_4$ structure viewed along different directions.

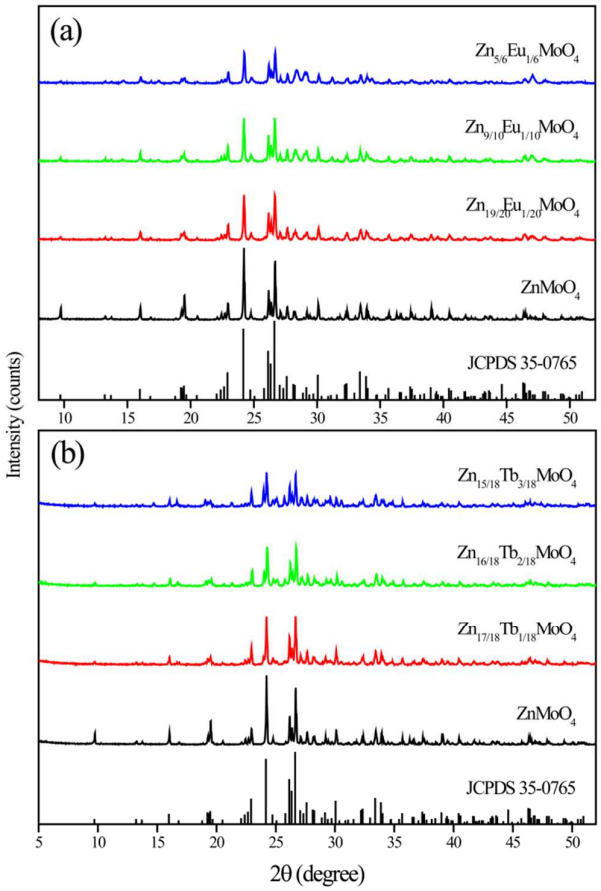

Fig. 3 (a): XRD patterns of the $ZnMoO_4$, $Zn_{0.95}Eu_{0.05}MoO_4$, $Zn_{0.90}Eu_{0.10}MoO_4$ and $Zn_{5/6}Eu_{1/6}MoO_4$ phosphors sintered at 700°C for 3h. (b): XRD patterns of the $ZnMoO_4$, $Zn_{17/18}Tb_{1/18}MoO_4$, $Zn_{8/9}Tb_{1/9}MoO_4$ and $Zn_{5/6}Tb_{1/6}MoO_4$ phosphors sintered at 800°C for 3h.

3.2 The identification of site occupancy preference.

The behaviours of luminescence centres are affected by host lattice environment. Covalence of chemical bond, coordination number of central ions and site symmetry appear to be important factors for the luminescence properties of Bi^{3+} ion.[21] Environmental factor of host lattice designated by the symbol h_e can be expressed as: $h_e = [\sum f_c(i)\alpha(i)Q(i)^2]^{1/2}$ where $f_c(i)$ is the fractional covalency of chemical bond from centre ion to ith ligand, $\alpha(i)$ is the polarizability of the ith chemical bond volume, $Q(i)$ is the charge presented by the ith neighbouring anion in the bond subformula, the number of sum terms equals to coordination number of the central ions.[22-23] The relationships between the positions of energy levels of Bi^{3+} and environmental factor h_e of host materials have been summarized and established in dozens of compounds. Energy levels of Bi^{3+} ion in crystals can be predicted according to the equation[24]: E_A=2.972+6.206exp(-h_e/0.551); E_C=3.236+10.924 exp(-h_e/0.644). It has been reported that Bi^{3+} $^1S_0 \rightarrow {}^3P_1$ transitions in $ZnWO_4$ and $CdWO_4$ are located at around 340 and 350 nm respectively. The refractive index n of $ZnMoO_4$ is already known[25] and chemical bond parameters can be calculated using dielectric theory of chemical bond for complex crystals. Making use of the refined structural parameters, h_e of three kinds of Zn sites in $ZnMoO_4$ were calculated and listed in Table 2. Then the positions of A band of Bi^{3+} in Zn(1), Zn(2) and Zn(3) sites are predicted to lie in 369 nm (27122 cm^{-1}), 331 nm (30184 cm^{-1}) and 340 nm (29368 cm^{-1}), respectively.

Table 2 Chemical bond parameters and h_e of three Zn sites in $ZnMoO_4$.

Bond type	$f_c(i)$	$\alpha(i)$	CN	$Q(i)$	h_e
Zn1-O1	0.6675	0.9734	1	0.8	
Zn1-O2	0.3939	0.8173	1	1.2	
Zn1-O4	0.3918	0.8465	1	1.2	1.5372
Zn1-O7	0.3841	0.9757	1	1.2	
Zn1-O12	0.3934	0.823	1	1.2	
Zn2-O4	0.2952	0.727	1	1	
Zn2-O6	0.5822	0.9725	1	0.66666	
Zn2-O7	0.3035	0.6149	1	1	1.1490
Zn2-O9	0.5808	0.9938	1	0.66666	
Zn2-O10	0.3095	0.5494	1	1	
Zn2-O10	0.2888	0.8339	1	1	
Zn3-O2	0.2972	0.6927	1	1	
Zn3-O3	0.5805	0.9948	1	0.66666	
Zn3-O5	0.582	0.9707	1	0.66666	1.2063
Zn3-O8	0.5801	0.9993	1	0.66666	
Zn3-O11	0.5773	1.0477	1	0.66666	
Zn3-O12	0.2946	0.7298	1	1	

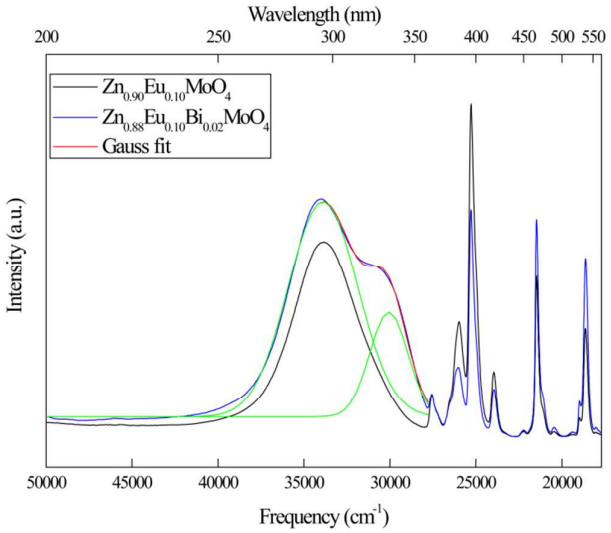

Fig. 4 PLE spectra of $Zn_{0.90}Eu_{0.10}MoO_4$ and $Zn_{0.88}Eu_{0.10}Bi_{0.02}MoO_4$ with an emission wavelength at 619 nm.

The excitation spectra of $Zn_{0.90}Eu_{0.10}MoO_4$ and $Zn_{0.88}Eu_{0.10}Bi_{0.02}MoO_4$ for monitoring Eu^{3+} $^5D_0 \rightarrow {}^7F_2$ (619 nm) emission were given in Fig. 4. The broad band at 250-310 nm (32258-40000 cm^{-1}) corresponds to the overlap of O^{2-}-Eu^{3+} and O^{2-}-Mo^{6+} charge transfer band. The sharp lines are due to the intra configurational 4f-4f transitions of Eu^{3+} ions, which can be assigned to $^7F_0 \rightarrow {}^5L_6$ (395 nm), $^7F_0 \rightarrow {}^5D_2$ (466 nm) and $^7F_0 \rightarrow {}^5D_1$ (537 nm), respectively. The asymmetric broad excitation band from 250-360 nm (40000-27777 cm^{-1}) of $Zn_{0.88}Eu_{0.10}Bi_{0.02}MoO_4$ was decomposed into two components by Gaussian fitting. Compared with the PLE spectrum of $Zn_{0.90}Eu_{0.10}MoO_4$, the excitation band at about 333 nm (30066 cm^{-1}) can be assigned to the $^1S_0 \rightarrow {}^3P_1$ transitions of the Bi^{3+}. Combined with the calculated results above, it can be concluded that the Bi^{3+} ions entered Zn(2) sites in the $ZnMoO_4$ and Zn(2) sites can be occupied preferentially.

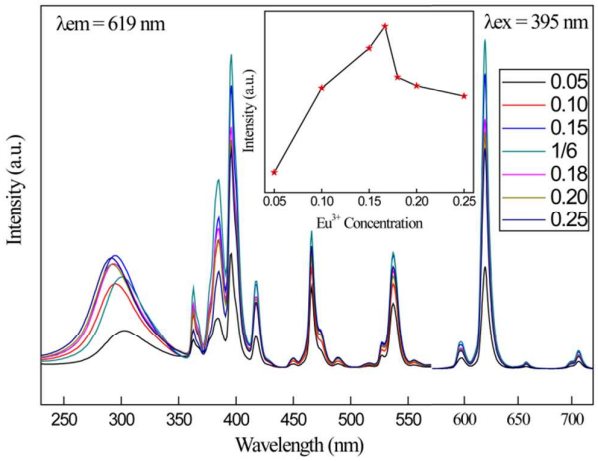

Fig. 5 Excitation and emission spectra of $Zn_{1-x}Eu_xMoO_4$ with different Eu^{3+} concentrations. The inset shows the dependence of emission intensity on the Eu^{3+}-doping concentration.

In order to optimize doping concentration of Eu^{3+}, a series of $Zn_{1-x}Eu_xMoO_4$ (x= 0.05, 0.10, 0.15, 1/6, 0.18, 0.20, 0.25) samples are synthesized, and the excitation and emission spectra of them are shown in Fig. 5. The broad excitation band from 250 to 350 nm monitoring Eu^{3+} 619 nm emission is the overlap of MoO_4^{2-} group absorption and charge transfer transition from O^{2-} to Eu^{3+}, which indicates that there exists efficient energy transfer from MoO_4^{2-} to the Eu^{3+} ions. In addition, the narrow bands at 395, 465, and 535 nm are attributed to f-f transitions of Eu^{3+}. In the PL spectra excited at 395 nm in Fig. 5, the emission bands at 596, 619, 657 and 706 nm are attributed to the transitions of $^5D_0 \rightarrow {}^7F_0$, $^5D_0 \rightarrow {}^7F_1$, and $^5D_0 \rightarrow {}^7F_2$ of Eu^{3+} ions respectively, with the strongest at 619 nm. The variation of $^5D_0 \rightarrow {}^7F_2$ emission intensity under 395 nm excitation is shown in the inset of Fig. 5. When excited at 395 nm, the emission intensity first increase with the increasing Eu^{3+} concentration x and then reach a maximum at x= 1/6. Concentration quenching occurs when the Eu^{3+} concentration is over 1/6, which is similar to the reported.[7, 19] Fig. 6 gives a possible quenching mechanism and when the concentration is beyond 1/6, two Eu^{3+} began to occupy the adjacent Zn(2) sites simultaneously (see Fig. 6(c)). The concentration quenching in $ZnMoO_4$ is due to the short distance of Zn(2) sites (3.2202 Å).

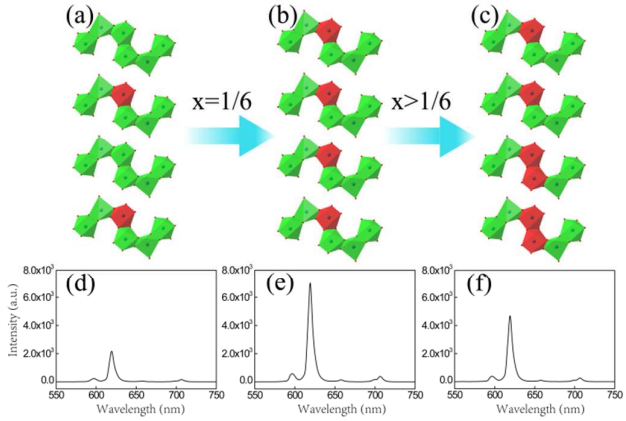

Fig. 6 Evolution of occupied Zn sites with the increasing Eu^{3+} concentrations: (a) x < 1/6; (b) x=1/6; (c) x > 1/6. (Red polyhedron represent occupied). Emission spectra of (d) $Zn_{0.95}Eu_{0.05}MoO_4$; (e) $Zn_{5/6}Eu_{1/6}MoO_4$ and (f) $Zn_{0.82}Eu_{0.18}MoO_4$ excited at 395 nm.

To verify the effect of site occupation preference in S-shaped cluster in $ZnMoO_4$ on concentration quenching, the doping concentration of Tb^{3+} ions optimization was performed. Fig. 7 presents the excitation and emission spectra of the $Zn_{1-x}Tb_xMoO_4$ (x=2/36, 4/36, 5/36, 6/36, 7/36, 8/36). The broad excitation band from 230 to 330 nm is ascribed to the overlap of the host absorption and charge transfer transition from O^{2-} to Tb^{3+}. The strong excitation bands at 377 and 487 nm are attributable to the $^7F_6 \rightarrow {}^5D_3$ and $^7F_6 \rightarrow {}^5D_4$ transitions of Tb^{3+}, respectively.[26-27] The dependence of the integrated emission intensity on the doped concentration of Tb^{3+} is shown in Fig. 7(b). A series of sharp lines in Fig. 7 (b) originates from intra-configurational 4f–4f transitions of Tb^{3+}, and the most intense emission band locates at 544 nm. The $^5D_3 \rightarrow {}^7F_j$ (j = 3, 4, 5, 6) transitions were not observed because of strong cross-relaxation of Tb^{3+} ions, i.e., Tb^{3+} ($^5D_3$) + Tb^{3+} ($^7F_6$)→Tb^{3+} ($^5D_4$) + Tb^{3+} ($^7F_0$). Concentration quenching occurs when the Tb^{3+} concentration is beyond 1/6, therefore the optimized concentration of Tb^{3+} in $ZnMoO_4$ is also 1/6. As shown in the inset in Fig. 7(b), the emission intensity increases with the increasing concentration x of Tb^{3+} and reaches a maximum at x=1/6, which is close to the reported.[18]

Therefore, we believe that the concentrate quenching occurred due to the same reason in $ZnMoO_4$:Tb^{3+}.

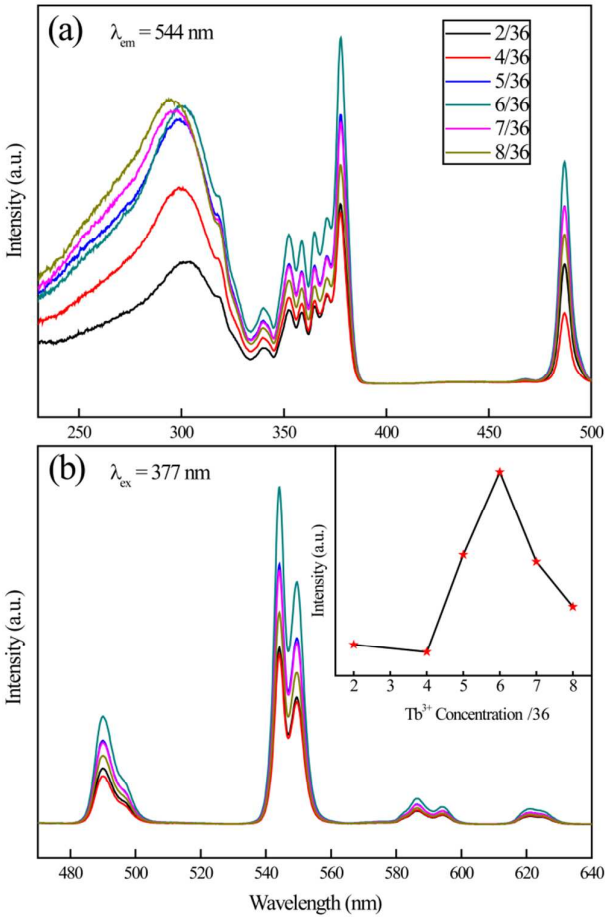

Fig. 7 The excitation (a) and emission (b) spectra of $Zn_{1-x}Tb_xMoO_4$ phosphors. The inset shows the dependence of emission intensity on the Tb^{3+}-doping concentration.

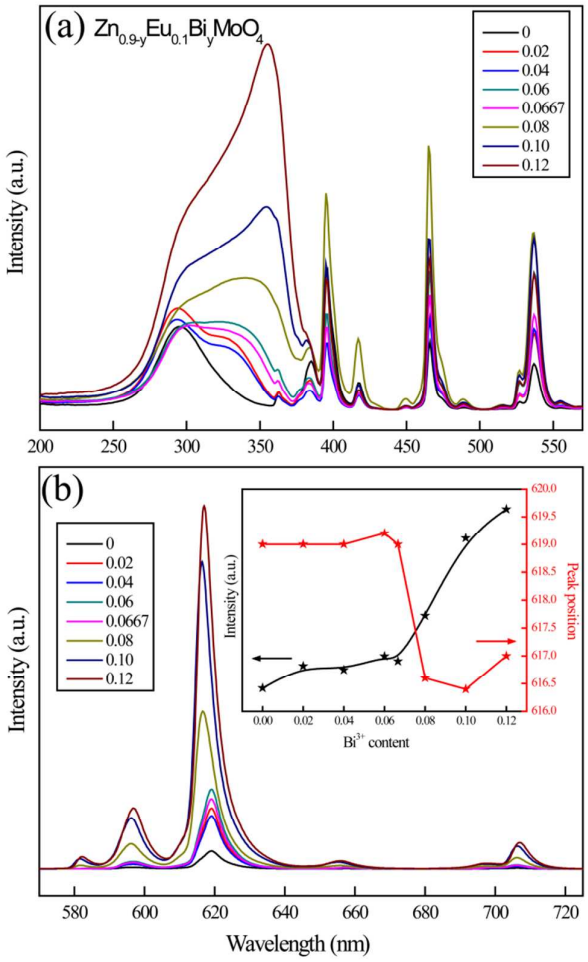

Fig. 8 The doping concentration dependent excitation and emission spectra of $Zn_{0.9-y}Eu_{0.1}Bi_yMoO_4$ (a and b).

3.3 Design and principle of super energy transfer process from Bi^{3+} to Eu^{3+} ions.

As an excellent sensitizer, Bi^{3+} ions can not only enhance the emission intensity, but also broaden the excitation bands.[28-29] According to the work above, concentration quenching occurs when Eu^{3+} or Tb^{3+} began to occupy the adjacent Zn(2) sites. Different from concentration quenching, for efficient energy transfer, the short distance between the sensitizers and activators is one basic condition.[30] When the total molar concentrations of Eu^{3+} and Bi^{3+} ions is beyond 1/6, they will occupy two adjacent Zn(2) sites (see Fig. 9(c)) and thus a super energy transfer from Bi^{3+} to Eu^{3+} is expected due to short distance between them. In order to investigate the influence of Bi^{3+} on luminescence properties, the variation of emission intensity in $Zn_{0.9-y}Eu_{0.1}Bi_yMoO_4$ phosphors with the increasing Bi^{3+} concentration is studied. Fig. 8(a) shows the excitation spectra of the $Zn_{0.9-y}Eu_{0.1}Bi_yMoO_4$ phosphors monitored at the $^5D_0 \rightarrow {}^7F_2$ transition emission (616-619 nm) of Eu^{3+}. Two strong excitation bands peaking at 295 nm and 331 nm correspond to O-Eu^{3+} CT and $^1S_0 \rightarrow {}^3P_1$ transitions of the Bi^{3+}, respectively. The intensity of excitation band at about 331 nm was enhanced remarkably when the total concentration of Eu^{3+} and Bi^{3+} ions is over

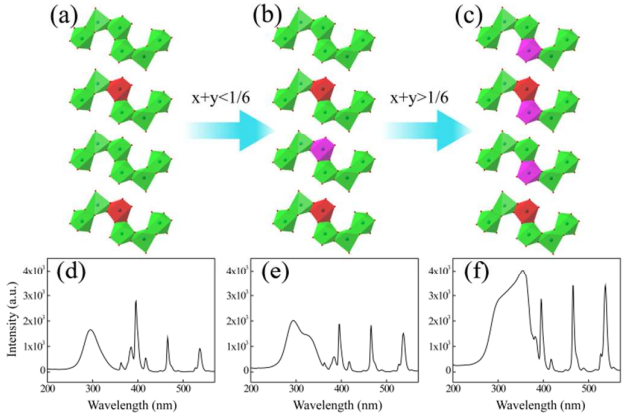

Fig. 9 Evolution of occupied Zn sites with the variation of Eu^{3+} and Bi^{3+} concentrations: (a) x < 1/6 and y=0; (b) x+y < 1/6 and y > 0; (c) x+y > 1/6 and y > 0. The central ion of red polyhedron is Eu^{3+}, and that of purple one is Bi^{3+}. Emission spectra of (d) $Zn_{0.95}Eu_{0.05}MoO_4$; (e) $Zn_{0.88}Eu_{0.10}Bi_{0.02}MoO_4$ and (f) $Zn_{0.80}Eu_{0.20}MoO_4$ monitored at Eu^{3+} ions $^5D_0 \rightarrow {}^7F_2$ emission (616-619 nm).

1/6. As shown in Fig. 8(b), when the concentration of Bi^{3+} is less than 0.06667, the intensity of Eu^{3+} $^5D_0 \rightarrow {}^7F_2$ emission increased slowly with the increasing Bi^{3+} concentration. When the Bi^{3+} content reaches 0.06667 the intensity becomes stronger sharply, indicating that the super energy transfer process was realized and it is illustrated in Fig. 9. More interestingly, when the total concentration is larger than 1/6, not only the emission intensity increased but also the peak position shifted. As Eu^{3+} and Bi^{3+} began to occupy two adjacent Zn(2) sites, the lattice environment was changed significantly. It caused the peak position of excitation band shifted from 331 nm to 355 nm obviously. The broad band excitation properties of $ZnMoO_4$:Bi^{3+}, Eu^{3+} in near UV region，as well as its pure red emission，makes it a promising red phosphor for white LEDs.

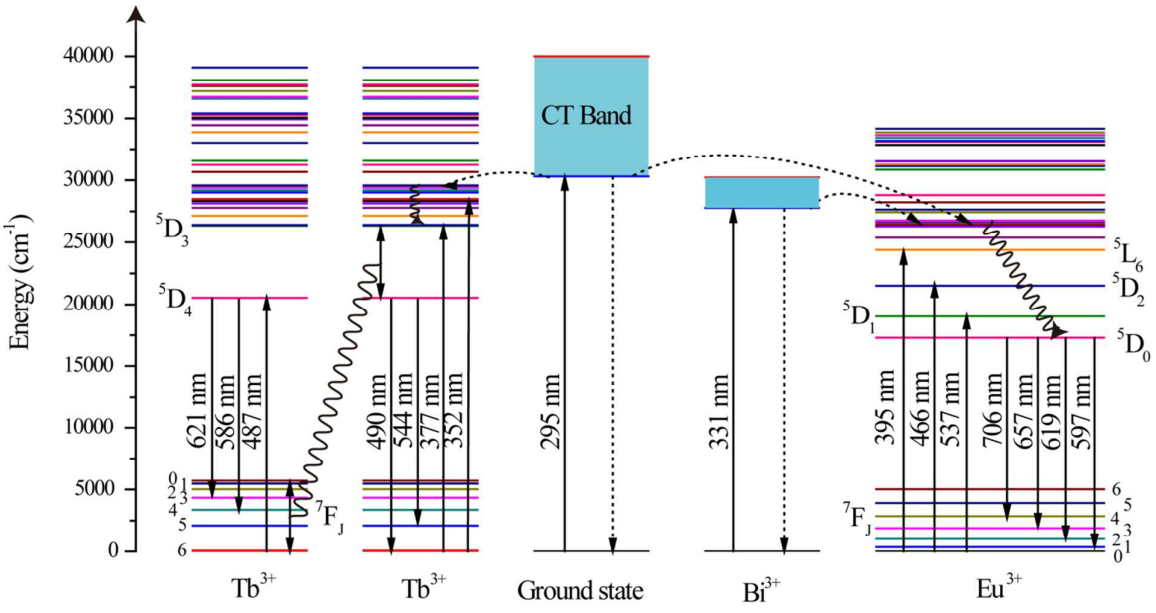

Fig. 10 The proposed energy transfer mechanisms in $ZnMoO_4$:Tb^{3+}, $ZnMoO_4$:Eu^{3+} and $ZnMoO_4$:Bi^{3+}/Eu^{3+}.

3.4 Energy Transfer Mechanism

Fig. 10 illustrates possible energy transfer process from charge transfer band to Eu^{3+} or Tb^{3+} and from Bi^{3+} to Eu^{3+} in $ZnMoO_4$. CT band can strongly absorb UV light at about 295 nm and then efficiently transfer the energy to $^5D_3$ level of Tb^{3+} ions. The emissions from $^5D_3 \rightarrow {}^7F_j$ (j = 3, 4, 5, 6) transitions were not observed due to the strong cross-relaxation of Tb^{3+}. Then a set of characteristic transitions $^5G_4 \rightarrow {}^7F_J$ situated at about 490, 544, 586 and 621 nm (J = 6, 5, 4 and 3) are exhibited. As Bi^{3+} ions being introduced into the $ZnMoO_4$:Eu^{3+}, its excitation band was significantly broadened, which due to the strong absorption of near-ultraviolet light and efficiently energy transfer from Bi^{3+} ions to Eu^{3+}.

4. Conclusions

In summary, a highly efficient near-UV excited red-emitting phosphor $ZnMoO_4$:Eu^{3+},Bi^{3+} with super energy transfer process was successfully designed and synthesized. In $ZnMoO_4$ crystal structure, every six Zn-O polyhedra compose an completely centrosymmetric S-shaped cluster by sharing edges. The environmental factor h_e of three kinds of Zn sites were calculated based on dielectric theory of chemical bond for complex crystals. Combined with our semi-empirical formula about Bi^{3+}, the position of A band of Bi^{3+} ions in three kinds of Zn sites were predicted to be Zn(1) 369 nm (27122 cm^{-1}), Zn(2) 331 nm (30184 cm^{-1}) and Zn(3) 340 nm (29368 cm^{-1}). The experimental results showed that the position of A band of Bi^{3+} lies in at about 333 nm (30066 cm^{-1}) and it proved that Zn(2) sites were replaced by Bi^{3+} ions. The site occupancy preference of doping ions in $ZnMoO_4$ is at the Zn(2) sites. The quenching concentration of single doped Eu^{3+} or Tb^{3+} ions in $ZnMoO_4$ was determined to be 1/6. When the single doping concentration is beyond 1/6, the concentration quenching occurs because two activators began to occupy the adjacent Zn(2) sites simultaneously. However, when the total concentration of Bi^{3+} and Eu^{3+} ions is large than 1/6, Bi^{3+} and Eu^{3+} ions began to occupy two adjacent Zn(2) sites respectively and the super energy transfer process occurred due to the short distance between Bi^{3+} and Eu^{3+}. A novel super energy transfer process with broad excitation band in near-UV region appeared in $ZnMoO_4$ phosphors. The relative intensity is about 6 times than the phosphor with ordinary transfer process. This work provides a new way of thinking in site occupation investigation and show a new angle on designing efficient phosphors.

Acknowledgements

This work is financially supported by Science and Technology Development Plan of Shandong Province, China (2014GNC110013) and Graduate Innovation Fund of Qingdao Agricultural University (QYC201422).

References

1. C. Feldmann, J. Thomas, R. R. Cees and J. S. Peter, *Adv Funct Mater*, 2003, **13**, 511-516.
2. S. Ye, F. Xiao, Y. Pan, Y. Ma and Q. Zhang, *Mat Sci Eng R*, 2010, **71**, 1-34.
3. S. Nakmura and G. Fasol, *The blue laser diode-GaN based light emitters and lasers*, Springer, Berlin, 1997. 216-221.
4. J.-M. Song, J.-S. Park and S. Nahm, *Ceram Int*, 2013, **39**, 2845-2850.
5. K. Hyo Sung, H. Takashi, H. Hiromasa and M. Ken-ichi, *J Phys Conf Ser*, 2012, **379**, 12016-12019.
6. P. Pust, V. Weiler, C. Hecht, A. Tücks, A. S. Wochnik, A.-K. Henß, D. Wiechert, C. Scheu, P. J. Schmidt and W. Schnick, *Nat Mater*, 2014, **13**, 891-896.
7. L.-Y. Zhou, J.-S. Wei, F.-Z. Gong, J.-L. Huang and L.-H. Yi, *J Solid State Chem*, 2008, **181**, 1337-1341.
8. L. Zhou, L. Yi, R. Sun, F. Gong and J. Sun, *J Am Ceram Soc*, 2008, **91**, 3416-3418.
9. J. Liu, H. Lian and C. Shi, *Opt Mater*, 2007, **29**, 1591-1594.
10. X. T. Wei, Y. H. Chen, X. R. Cheng, M. Yin and W. Xu, *Applied Physics B*, 2010, **99**, 763-768.
11. Z. G. Xia, D. M. Chen, M. Yang and T. Ying, *J Phys Chem Solids*, 2010, **71**, 175-180.
12. S. X. Yan, J. H. Zhang, X. Zhang, S. Z. Lu, X. G. Ren, Z. G. Nie and X. J. Wang, *J Phys Chem C*, 2007, **111**, 13256-13260.
13. R. A. Benhamou, A. Bessière, G. Wallez, B. Viana, M. Elaatmani, M. Daoud and A. Zegzouti, *J Solid State Chem*, 2009, **182**, 2319-2325.
14. S.-S. Wang, W.-T. Chen, Y. Li, J. Wang, H.-S. Sheu and R.-S. Liu, *J Amer Chem Society*, 2013, **135**, 12504-12507.
15. J. Shi, L. Wang, Q. Sun, Q. Wei, L. Cui and Y. Hu, *J Electrochem Soc*, 2011, **158**, 136-139.
16. M. Peng, X. Yin, P. A. Tanner, M. G. Brik and P. Li, *Chem Mater*, 2015, **27**, 2938-2945.
17. T. Chengaiah, C. K. Jayasankar, K. Pavani, T. Sasikala and L. R. Moorthy, *Opt Commun*, 2014, **312**, 233-237.
18. X. Ju, X. Li, W. Li, W. Yang and C. Tao, *Mater Lett*, 2011, **65**, 2642-2644.
19. A. Xie, X. Yuan, F. Wang, Y. Shi and Z. Mu, *J Phys D Appl Phys*, 2010, **43**, 55101-55105.
20. W. Reichelt, T. Weber, T. Söhnel and S. Däbritz, *Z Anorg Allg Chem*, 2000, **626**, 2020-2027.
21. L. I. Van Steensel, S. G. Bokhove, A. M. Van der Craats, J. De Blank and G. Blasse, *Mater Res Bull*, 1995, **30**, 1359-1362.
22. F. Gao and S. Zhang, *J Phys Chem Solids*, 1997, **58**, 1991-1994.
23. J. Shi and S. Zhang, *J Phys: Condens Mat*, 2003, **15**, 4101.
24. L. L. Wang, Q. Sun, Q. Z. Liu and J. S. Shi, *J Solid State Chem*, 2012, **191**, 142-146.
25. A. E. Savon, D. A. Spassky, A. N. Vasil'ev and V. V. Mikhailin, *Opt Spectrosc+*, 2012, **112**, 72-78.
26. Q. Guo, L. Liao and Z. Xia, *J Lumin*, 2014, **145**, 65-70.
27. J. Liao, D. Zhou, X. Qiu, S. Liu and H.-R. Wen, *Optik*, 2013, **124**, 5057-5060.
28. W. Ran, Q. Wang, Y. Zhou, S. Ding, J. Shi and J. H. Jeong, *Mater Res Bull*, 2015, **64**, 146-150.
29. W. Ran, L. Wang, H. Li, Y. Guo, W. Kang, D. Qu, J. Shi and L. Su, *Ceram Int*, 2015, **41**, 4301-4307.
30. H. Zhu, Z. Xia, H. Liu, R. Mi and Z. Hui, *Mater. Res. Bull*, 2013, **48**, 3513-3517.

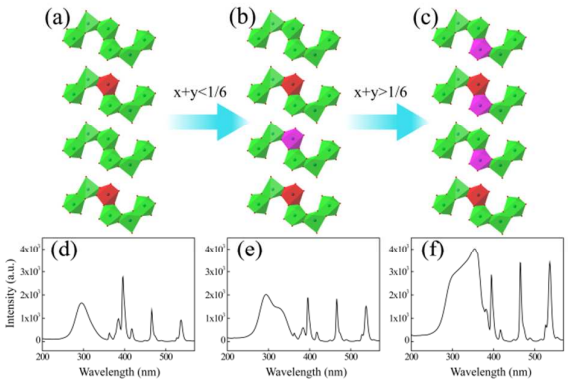

In $ZnMoO_4$ phosphor, Bi^{3+} and Eu^{3+} ions were trapped together in the S-shaped cluster. The super energy transfer process from Bi^{3+} to Eu^{3+} occurred due to their short distance.